BULETINUL Universităţii Petrol – Gaze din Ploieşti	Vol. LVIII No. 2 bis / 2006	273-280	Seria Tehnică

Some Aspects Concerning the Magnetic Field Computation for the Reluctance Motor With Axially-Laminated Rotor

Ileana Torac[*], Alin Argeşeanu[**]

[*] Romanian Academy-Timisoara ,
e-mail ileana_torac@yahoo.com
[**]"Politehnica" University Timisoara,
e-mail: alin_argeseanu@yahoo.com

Abstract

The paper deals with the analytical computation of the air-gap flux density and of the inductance, for the reluctance motor with axially laminated rotor. The non-linearity of the steel laminations is taken into account for both d- and q-axis field. One had considered as known the motor data (geometrical dimensions, winding data, B-H curve of the ferromagnetic material) and the stator phase current. The good correspondence of the calculated and measured values of the magnetizing inductance validates the proposed method.

Key words: *reluctance machine, analytical method, axially laminated rotor.*

Introduction

The performances of the synchronous reluctance motor are essentially dependent on the magnetic dissymmetry of its rotor [1],[2],[3]. The last one is made from grain-oriented steel laminations, alternating with insulation and non-magnetic material (see Fig. 1). The fastening is realized with clamping plates and screws made from non-magnetic material (brass or non-magnetic stainless-steel), to avoid the increase of the q-axis reluctance. Both width of the clamping plates and domain occupied of screws depend on the rotor dimensions and on the number of pole pairs.

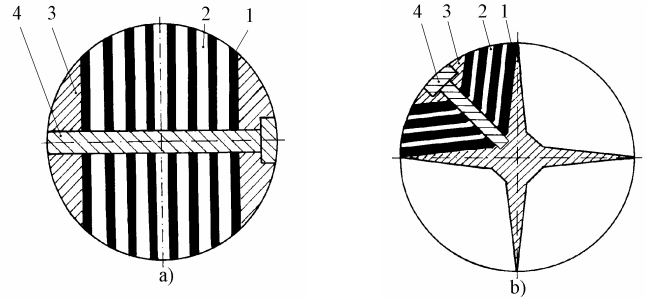

1. laminations; 2. insulation sheet 3. clamping plates 4. non-magnetic stainless steel bolt

Fig.1. Example of rotor shape: (a) two-pole machine; (b) four-pole machine.

Using the program based on the method presented below, one can analyze any axially rotor shape having more than 3 lamination and more than 2 insulation sheets.

Simplifying hypothesis

One agrees that in all the cross sections of the machine the magnetic field is the same; one neglects the magnetic field, which closes through the front area.
One considers the m.m.f. having a sinusoidal distribution on the inner surface of the stator.
The influence of stator slots is taken into account by the Carter factor; the influence of the insulation sheets is considered, as in [3].
One neglects the presence of the non-magnetic stainless-steel bolts.
One considers the non-linearity of the steel laminations for both d- and q-axis field computation.
One considers that the q-axis field between two adjacent steel laminations of the rotor is a plan-parallel one.

The equivalent air-gap computation in the area of the clamping plates

Concerning the shape variation of the air gap along the pole pitch, one can emphasize two areas: one corresponding to the rotor area composed of laminations and insulation sheets, the other corresponding to the clamping plates area.
The clamping plates have the thickness approximately 10 times bigger as the laminations, because of mechanical strength conditions. One computes the equivalent air-gap corresponding to this non-magnetic area as in [3]:

$$\delta(x) = \delta + \delta_{cx} \tag{1}$$

where δ is the "geometrical" air gap length and δ_{cx} depends on the following quantities: p –the number of pole pairs, r –the rotor radius, δ_c – the clamping plates width.

The calculation of the d-axis air gap flux density

Considering as known the machine data (geometrical dimensions, B-H curve of the ferromagnetic material) and the stator m.m.f. distribution on the inner stator surface, one can obtain the d-axis flux density distribution in the air gap, $B_{\delta d}(x)$.
Fig. 2 presents the approximate field line, in order to compute the m.m.f. in the case of a two-pole machine.
For any field line, the m.m.f. corresponding to each section of the magnetic circuit (air gap, stator yoke, stator tooth and ferromagnetic rotor area) depends on the value of the flux density in the air gap point M, crossed by the considered field line.
The coordinate $\boldsymbol{x}$ defines the position of the point M relating to the d-axis.
One divides the motor air gap into sections where the flux density is considered the same, having the value corresponding to the point in the middle of the section. The number of points where the flux density is computed depends on the difference accepted between $B_{\delta d}$ values for two adjacent sections. For lamination width less than 1 mm, one considers a single point straight to each lamination
For the considered point one gives as initial value the $B_{\delta d}(x)$ that corresponds to the case $\mu_{fe} \to \infty$.

$$B_{\delta l}(x) = \frac{\theta_d(x)}{\delta_\lambda}\mu_0 \tag{2}$$

With this value one computes the magneto-motive force for each section of the magnetic circuit.

The computed resultant m.m.f. considering μ_{fe} finite, became greater than $\theta(x)$ initially considered and then a new value is given for the air gap flux density.

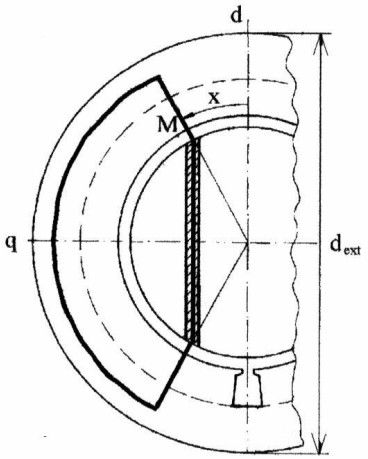

Fig. 2. The approximate field line for a two-pole machine.

The iterative process continues until the difference between the computed values of the m.m.f. and the initial admitted value is smaller than the fixed error.

In air gap area corresponding to the rotor part composed of lamination and insulation sheets, one considers a single point straight to each lamination for the flux density calculus, because the lamination width is usually less than 1 mm. As result, for this air gap area one computes the flux density for a number of points equal to the laminations number, n.

In the second air gap area, corresponding to the clamping plates, the flux density obtains a low value (because of the high value of the air gap width, due to the clamping plates), so it is not affected by the non-linearity of the ferromagnetic material. Therefore, one computes the flux density for n_c points, n_c being less than n.

One obtains the air-gap flux density distribution along a half pole pitch (Fig. 3). With these $n+n_c$ values one can compute the amplitude of the fundamental of the d-axis air gap flux density:

$$B_{\delta d1} = \frac{4}{\pi}\left[\sum_{\lambda=1}^{n} B_{\delta\lambda}\left(\sin\frac{x_{\lambda f}}{\tau}\pi - \sin\frac{x_{\lambda i}}{\tau}\pi\right) + \sum_{k=1}^{n_c} B_{\delta k}\left(\sin\frac{x_{ki}}{\tau}\pi - \sin\frac{x_{kf}}{\tau}\pi\right)\right] \tag{3}$$

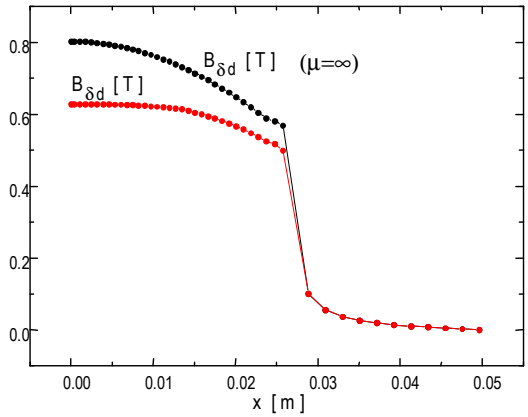

Fig. 3. The d-axis flux density distribution along a half pole pitch (between d and q- rotor axis).

Fig. 3 presents the d-axis flux density distribution along the half pole pitch, between d and q axis of the rotor, for two cases: considering the non-linearity of the ferromagnetic circuit and considering $\mu_{fe} \to \infty$. The motor has the following data: P = 0.55kW, p = 1, I = 1A, 59 rotor insulation sheets, 0.22mm width of the insulation sheets and 0.5mm width of the rotor lamination.

The calculation of the q-axis air gap flux density

The q-axis air gap flux density is computed using the magnetic circuit law and the magnetic flux law. The variable λ defines the position of the considered lamination relating to the d-axis of the rotor. The considered rotor shape has the first rotor lamination (labeled λ=1) placed in the d-axis. Figure 4 presents the rotor laminations λ and λ+1.

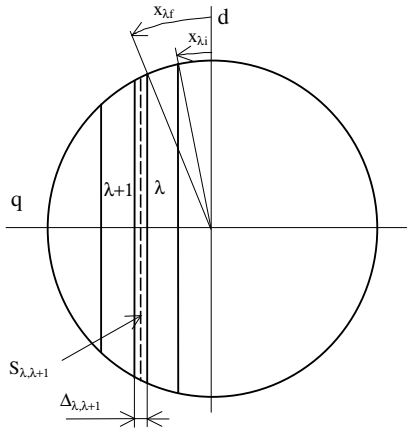

Fig. 4. Explanatory for the q-axis field computation.

The insulation sheet width is $\Delta_{\lambda,\lambda+1}$.
The q-axis air gap flux density $B_{\delta q}(x)$ straight to the λ lamination is:

$$B_{\delta q}(x) = \mu_0 \frac{\theta_q(x) - V_\lambda}{\delta_\lambda} \tag{4}$$

According to the last simplifying hypothesis, one considers that the magnetic scalar potential of every rotor lamination, is:

$$V_\lambda(x) = v_\lambda x \tag{5}$$

The q-axis flux which crosses any lamination λ (λ=1,2,…,n-1) has two terms: the q-axis flux $\Phi_{\lambda+1}$, penetrating from lamination λ+1 through the insulation sheet, and the q-axis flux, which penetrates from the air gap (through the area limited by the coordinates $x_{\lambda i}$ and $x_{\lambda f}$).

$$\Phi_\lambda = \Phi_{\lambda+1} + 2\mu_0 l \int_{x_{\lambda i}}^{x_{\lambda f}} \frac{\theta_q(x) - v_\lambda x}{\delta_\lambda} dx \tag{6}$$

Only for λ=n, the equation (6) of the q-axis flux, which penetrates the lamination, has a single term, the flux penetrating from the air gap.
For each insulation sheet placed between the laminations λ and λ+1 one can write the magnetic circuit law:

$$v_{\lambda+1} x_{\lambda+1,i} - v_\lambda x_{\lambda f} = \Phi_{\lambda+1} \frac{\Delta_{\lambda,\lambda+1}}{S_{\lambda,\lambda+1}} \frac{1}{\mu_0} \tag{7}$$

For every rotor lamination one can write:

$$v_\lambda x_{\lambda i} - v_\lambda x_{\lambda f} = \Phi_\lambda \frac{\Delta_\lambda}{S_\lambda} \frac{1}{\mu_\lambda} \tag{8}$$

Writing equations as (6),(7) and (8) for all the **n** laminations and **n-1** insulation sheets (λ=1,2…n), one obtains a system having **2n** equations and **2n** unknown quantities: **n** values for the q-axis flux Φ_λ and **n** values for the constant v_λ defining the magnetic scalar potential $V_\lambda(x)$.
Obviously, the value of lamination permeability is different for every lamination. The magnetic stress corresponds to the total field. Therefore, one considers the initial values of μ_λ these corresponding to the d-axis field.
In order to solve the system using an iterative algorithm, the relations for the magnetic fluxes and for the magnetic scalar potential were transformed as follows:

$$\Phi_\lambda = C_{\Phi_\lambda \theta}\theta + C_{\Phi_\lambda V_n} V_n \tag{9}$$

$$V_\lambda = C_{V_\lambda \theta}\theta + C_{V_\lambda V_n} V_n \tag{10}$$

The coefficients $C_{\Phi_\lambda \theta}, C_{\Phi_\lambda V_n}, C_{V_\lambda \theta}, C_{V_\lambda V_n}$ depend only on the geometrical and material data.

The value of the equivalent air-gap corresponding to the q-axis produces a low value of the magnetic field, in comparison to that corresponding to the d-axis.
Solving this system one obtains the q-axis flux and the magnetic scalar potential for each lamination, depending on the geometrical data, on the amplitude of the stator m.m.f., on the magnetic permeability of the air gap and that of the rotor laminations. With this values one can estimate the air gap flux density $B_{\delta q}(x)$ straight to each lamination.
The presented calculus takes into account only the m.m.f. corresponding to the air gap and to the rotor area and the results depend on the ferromagnetic permeability of the stator and rotor laminations. Therefore, it is necessary an iterative calculus for the final values of the q-axis flux density. One divides the motor air gap into sections where the flux density is considered the same, having the value corresponding to the point in the middle of the section. One can consider a single point straight to each lamination.
For the considered point one gives as initial value the $B_{\delta q}(x)$ that corresponds to the solution obtained from (4),(6), (7), (8).
One begins with the point placed straight to the first rotor lamination because his magnetic scalar potential has the lowest value ($V_1(0)=0$).
With the considered value of $B_{\delta q}(x)$ one computes the m.m.f. for each section of the magnetic circuit of the stator (teeth and yoke) and of the rotor (laminations and insulation sheets).
The rotor section of a field line crossing the air gap at the distance x_λ relating to the d-axis of the rotor is presented in Fig. 5.

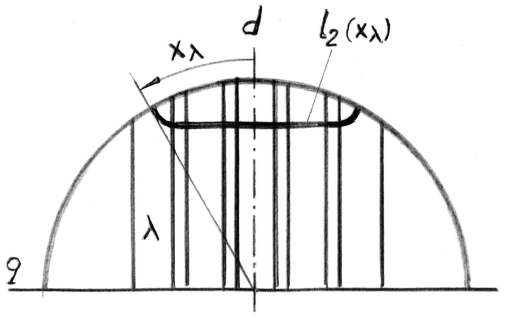

Fig. 5. The field line in the rotor area.

The computed resultant m.m.f. becomes greater than θ(x) initially considered and then a new value is given for the q-axis air gap flux density. The iterative process continues until the difference between the computed value of the m.m.f. and the initial admitted value is smaller than the fixed error.

As it is known, a satisfactory value of the saliency ratio requires a lamination thickness under 1 mm. Therefore, in the first air gap area (straight to the rotor part composed of lamination and insulation sheets), one considers a single point straight to each lamination for the flux density calculus. As result, for this air gap area one computes the flux density for a number of points equal to the laminations number, n.

In the second air gap area (straight to the clamping plates), one computes the flux density for n_c points, n_c being less than n.

The distribution of the q-axis air gap flux density along a half pole pitch, between the d and q-axis (for the case $\mu_{fe}\rightarrow\infty$), is presented in Fig.6.

The amplitude of the fundamental of the q-axis flux density in the air gap is obtained from the following equation:

$$B_{\delta q1}=\frac{4}{\pi}\left[\sum_{\lambda=1}^{n}B_{\delta\lambda}\left(\sin\frac{x_{\lambda f}}{\tau}\pi-\sin\frac{x_{\lambda i}}{\tau}\pi\right)+\sum_{k=1}^{n_c}B_{\delta k}\left(\sin\frac{x_{ki}}{\tau}\pi-\sin\frac{x_{kf}}{\tau}\pi\right)\right] \tag{11}$$

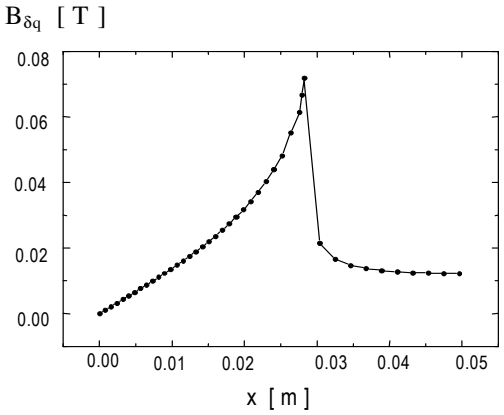

Fig. 6. The q-axis flux density distribution along a half pole pitch (between d and q- rotor axis).

The magnetizing inductance computation

The magnetic flux and the d-axis magnetizing inductance corresponding to $B_{\delta d1}$ are computed in (12) and (13):

$$\Phi_{d1}=\frac{8}{\pi^2}l\tau\left[\sum_{\lambda=1}^{n}B_{\delta\lambda}\left(\sin\frac{x_{\lambda f}}{\tau}\pi-\sin\frac{x_{\lambda i}}{\tau}\pi\right)+\sum_{k=1}^{n_c}B_{\delta k}\left(\sin\frac{x_{ki}}{\tau}\pi-\sin\frac{x_{kf}}{\tau}\pi\right)\right] \tag{12}$$

$$L_{md1}=\frac{2}{\pi}m(Nk_b)^2\frac{\Phi_{d1}}{\theta} \tag{13}$$

With the amplitude of the fundamental of the q-axis air gap flux density, $B_{\delta q1}$, one computes the magnetic flux Φ_{q1} and the magnetizing inductance L_{mq1}, corresponding to the q-axis, as follows:

$$\Phi_{q1} = \frac{8}{\pi^2} l\tau \left[\sum_{\lambda=1}^{n} B_{\delta\lambda} \left(\sin \frac{x_{\lambda f}}{\tau}\pi - \sin \frac{x_{\lambda i}}{\tau}\pi \right) + \sum_{k=1}^{n_c} B_{\delta k} \left(\sin \frac{x_{ki}}{\tau}\pi - \sin \frac{x_{kf}}{\tau}\pi \right) \right] \tag{14}$$

$$L_{mq1} = \frac{2}{\pi} m (N k_b)^2 \frac{\Phi_{q1}}{\theta} \tag{15}$$

where:

k_b - winding factor; l - length of the stack; m - number of phases; N - number of turns per phase; μ_0 - vacuum permeability; θ - amplitude of m.m.f.;

Based on this method one had developed a computing program for the air-gap flux density and magnetizing inductance estimation. One considers as input quantities the motor data (geometrical dimensions, winding data, B-H curve of the ferromagnetic material) and the stator phase current. One had used the program to analyze a two-pole machine with axially laminated rotor. All the insulation sheets have the same width, Δ_{iz} ; the lamination width is Δ_{fe}.

Computing the magnetizing inductance for different values of the phase current I one obtain the variation $L_{md1}(I)$ and $L_{mq1}(I)$.

The paper deals not with the computation of the leakage inductance.

For the same motor data, a finite element method based program [4], gives the results presented in Fig. 8. and Fig. 9. respectively. The flux density distribution in the machine cross section, presented in Fig. 8., is obtained with the finite element method. The f.e.m. gives the air–gap flux density along the pole pitch (Fig. 9) while the analytical method can give each component corresponding to d- and q-axis. Note the running time about a few hours, for a satisfactory accuracy of the calculus using the f. e. m. based program.

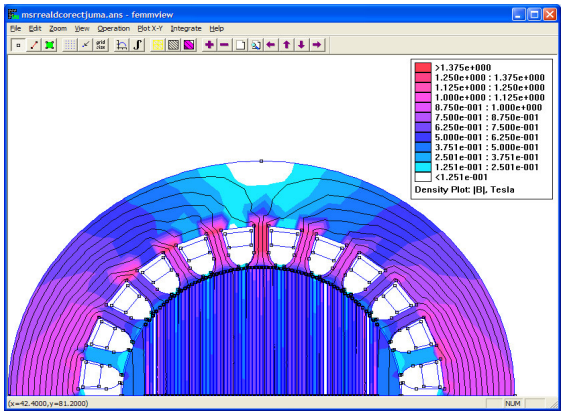

Fig. 8. The flux-density distribution.

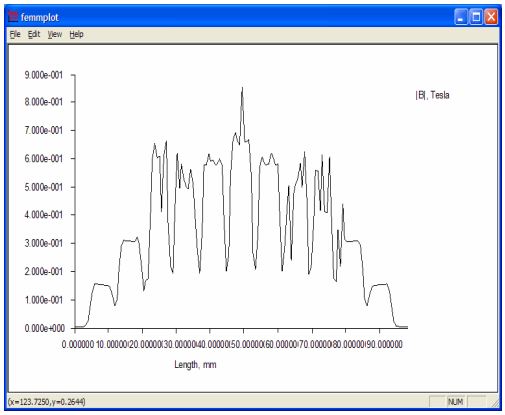

Fig. 9. The air-gap flux density along a pole pitch.

Experimental results

The magnetizing inductance validation was realized using the d.c. decay test [1], [2], [5].

Measurements are made using an acquisition system composed of: current transducers LA 55P, voltage transducers LV 25V, D/A interface, type PC+, PC 586, 133 MHz, 8MB RAM, and acquisition soft.

The tested motor has the rated power 0.55kW, the supply frequency 50Hz, the phase voltage 110V, the number of poles 2 and 59 insulation sheets.

The variation of the magnetizing inductance, L_{md1} and L_{mq1} on the phase current. I, are presented in Fig. 9 and Fig. 10 respectively.

One finds a satisfactory correspondence between the computed and measured values of the magnetizing inductances.

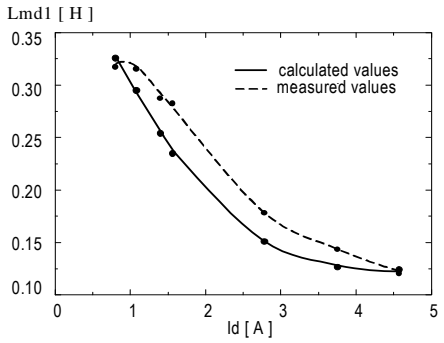

Fig. 9. Variation L_{md1} (I_d)**.**

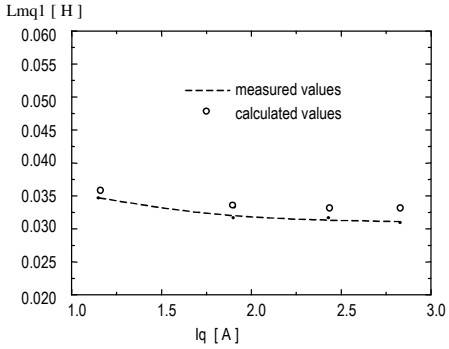

Fig. 10. Variation L_{mq} (I_q).

Conclusions

The paper presents an analytical method for the theoretical determination of the air gap flux density respectively of magnetizing inductances, for the synchronous reluctance motor with axially laminated rotor.

For the magnetizing inductances one finds a satisfactory correspondence between the computed and the measured values. Experimental results of a 0.55kW tested motor validate the proposed analytical method for design and optimization purposes.

The running time of the used program is significantly shorter in comparison to the finite element method based program. Therefore one can analyze a large combination of the rotor data (width and number of the insulation sheet and of the lamination) in order to obtain the required motor performances.

References

1. B o l d e a , I . - *Reluctance synchronous machines and drives*, Clarendon Press, Oxford, 1996.
2. B o l d e a , I . - *Electric machine parameters - identification, estimation and validation*, Ed. Academiei Romane, Bucuresti, 1999
3. T o r a c , I . - *An analytical model of the synchronous reluctance machine with axially-laminated rotor*, Ph.D. thesis, Universitatea "Politehnica" Timisoara, 1999.
4. M e e k e r , D . - *Finite Element Method Magnetics*, User's manual, 1999
5. V a s , P . - *Parameter estimation, condition monitoring and diagnosis of electrical machines,* Clarendon Press, Oxford, 1993

Aspecte privind calculul câmpului la motorul reactiv cu rotor stratificat

Rezumat

În lucrare se prezintă o metodă analitică de calcul a inductiei magnetice în întrefier şi a inductivităţilor motorului reactiv cu rotor stratificat, în funcţie de datele maşinii şi de mărimile de material. Concordanţa bună între valorile estimate şi cele măsurate ale inductivităţilor confirmă utilitatea metodei propuse.